

A novel dual-stage algorithm for capacitated arc routing problems with time-dependent service costs

Qingya Li^a, Shengcai Liu^a, Juan Zou^{b,c}, Ke Tang^a

^aGuangdong Key Laboratory of Brain-Inspired Intelligent Computation, Department of Computer Science and Engineering, Southern University of Science and Technology, Shenzhen 518055, China

^bThe Key Laboratory of Hunan Province for Internet of Things and Information Security, Xiangtan University, Xiangtan 411105, China

^cThe Key Laboratory of Intelligent Computing and Information Processing, Ministry of Education, Xiangtan University, Xiangtan 411105, China

Abstract

This paper focuses on solving the capacitated arc routing problem with time-dependent service costs (CARPTDSC), which is motivated by winter gritting applications. In the current literature, exact algorithms designed for CARPTDSC can only handle small-scale instances, while heuristic algorithms fail to obtain high-quality solutions. To overcome these limitations, we propose a novel dual-stage algorithm, called MAENS-GN, that consists of a routing stage and a vehicle departure time optimization stage. The former obtains the routing plan, while the latter determines the vehicle departure time. Importantly, existing literature often ignores the characteristic information contained in the relationship between the route cost and the vehicle departure time. The most significant innovation in this paper lies in the exploitation of this characteristic information during the vehicle departure time optimization stage. Specifically, we conduct a detailed analysis of this relationship under various scenarios and employ tailored methods to obtain the (approximately) optimal vehicle departure time. Furthermore, we propose an improved initialization strategy that considers time-dependent characteristics to achieve better solution quality. In addition to the modified benchmark test sets, we also experiment on a real-world test set. Experimental results demonstrate that MAENS-GN can obtain high-quality solutions on both small-scale and larger-scale instances of CARPTDSC.

Keywords:

Capacitated arc routing problem, Time-dependent service costs, Vehicle departure time, Memetic algorithm, Combinatorial optimization

1. Introduction

The arc routing problem (ARP) is a complex planning and scheduling problem commonly found in operations research, transportation, and industrial applications [1]. Among ARPs, the capacitated arc routing problem (CARP) is the most representative form with capacity constraints [2]. CARP is widely applied in numerous practical scenarios, such as winter gritting applications [3], urban waste collection [4, 5], street sweeping [6], and electric meter reading [7]. As a combinatorial optimization problem, CARP requires determining the least-cost routing plan for vehicles to serve all tasks subject to certain constraints [2]. CARP is generally described by a directed graph in which each task is associated with an arc. Arcs with tasks that must be served are terms required arcs, and each required arc is associated with a service cost and a demand. Arcs without tasks are called deadhead or travel arcs, which do not require service. Each travel arc is always associated with a travel cost. If certain information, such as service cost, travel cost, or demand, varies with time, then the problem becomes the time-dependent capacitated arc routing problem (TDCARP). Among TDCARPs,

the CARP with time-dependent service costs (CARPTDSC) is common in real-life scenarios.

CARPTDSC is motivated by winter gritting or salting applications [8, 9]. In this scenario, a fleet of fully loaded trucks, carrying deicing material (like salt), is dispatched to remove snow from critical roads in the urban road network. The objective is to determine the routing plan and the vehicle departure time that minimizes the total cost while serving all tasks. Each task is specified for a road from which a truck must remove snow by salting. The service cost of each task is defined as the consumption of time or deicing material when serving the task. However, this consumption always varies depending on the time at which the service begins for a particular road, due to factors like traffic, temperature, and weather conditions. Therefore, the time of beginning of service for a task affects its service cost, making the service cost time-dependent. In [8, 10], the relationship between the service cost of each task and its time of beginning of service is modeled as a three-segment linear function, as depicted in Fig. 2(a). In this case, if the task is served at the optimal time point or interval (i.e., $[bt, et]$ in Fig. 2(a)), the service cost is minimal. If service begins earlier or later than this time point or interval, the service cost of the task will increase dramatically. For convenience, in [9], the relationship is modeled as a two-segment linear function, as

Email addresses: liqy2020@mail.sustech.edu.cn (Qingya Li), liusccc@gmail.com (Shengcai Liu), zoujuan@xtu.edu.cn (Juan Zou), tangk3@sustech.edu.cn (Ke Tang)

shown in Fig. 2(b), which is a degenerate form of the three-segment linear function. In this case, the service cost is lowest when the service starts at time 0, although this rarely happens in real life [9]. Based on the types of time-dependent functions, CARPTDSC can be classified into two-segment linear function problems (abbreviated as 2LP) and three-segment linear function problems (abbreviated as 3LP).

For the 2LP, the variable neighborhood descent heuristic (VND) [9] has been proposed, but it has been observed to be less effective. On the other hand, for the 3LP, an exact algorithm [8] has been proposed, which however is only capable of handling small-scale problem instances (number of tasks ≤ 40). Motivated by these limitations, this paper investigates two research questions:

RQ1 For the 2LP, the quality of the approximate solutions obtained by the existing algorithm is not high, how to further enhance the quality of the solutions?

RQ2 For the 3LP, the existing algorithm is limited to solving small-scale instances, how to effectively address larger-scale instances?

To address the aforementioned research questions, we propose a novel dual-stage algorithm. Given that CARPTDSC involves two types of decision variables, namely the routing plan X and the vehicle departure time T , the two stages of the proposed algorithm align with solving for these decision variables, respectively. Consequently, the dual stages are denoted as the routing stage and the vehicle departure time optimization stage, respectively. In the routing stage, the primary focus is on obtaining a routing plan X by modifying the memetic algorithm with extended neighborhood search (MAENS) [2]. On the other hand, the vehicle departure time optimization stage concentrates on determining the vehicle departure time corresponding to each route in X using the golden section search (GSS) [11] or negatively correlated search (NCS) [12]. As a result, the proposed algorithm is termed MAENS-GN. The contributions made in this paper are briefly summarized as follows.

- When optimizing for vehicle departure time, existing works have ignored the characteristic information embedded in the relationship between the route cost and the vehicle departure time. To exploit this information to improve performance, we conduct a detailed analysis of the relationship across different scenarios. Based on the relationships analyzed in different scenarios, tailored approaches are adopted.
- An improved initialization strategy that considers time-dependent characteristics is proposed to enhance the effectiveness.
- Experiments were conducted on both modified standard test sets and a test set derived from real-world applications in Jingdong Logistics. The experimental results demonstrate that MAENS-GN yields positive effectiveness, indicating that this algorithm has addressed two research questions well.

The rest of this paper is organized as follows. Section 2 introduces the background and related work. Section 3 describes the proposed algorithm, i.e., MAENS-GN. After that, experimental studies are presented in Section 4. Finally, Section 5 presents the conclusion and future work.

2. Background and related work

In this section, the definition of CARPTDSC is first introduced. Then, the static algorithm MAENS [2], especially its initialization strategy, is described. Finally, we introduce the related work.

2.1. Problem definition

$G = (V, A)$ is a directed graph where V is the set of vertices and A denotes the set of arcs. Each arc $e \in A$, which can be represented as $e = \langle i, j \rangle$, and $i, j \in V$. i, j represent the tail node and head node of arc e , respectively. A can be partitioned into two subsets, namely A_1 and A_2 . $A_1 \subseteq A$ denotes the set of required arcs, also known as the set of tasks, each of which must be served. Each required arc is assigned a unique ID, which is set to the positive integer. $A_2 \subseteq A$ represents the set of travel or deadhead arcs, each of which does not need to be served and is used only for a traveling action. Each required arc $re \in A_1$ is associated with a demand $d(re)$, a length len_{re} , a deadhead or travel time dt_{re} , a service time st_{re} , a deadhead or travel cost DC_{re} , and a time-dependent piecewise linear service cost function $SC(re, T_{re})$, where T_{re} denotes the time of beginning of service on required arc re . Each travel arc $de \in A_2$ is associated with a length len_{de} , a travel time dt_{de} , and a travel cost DC_{de} .

K identical vehicles with capacity Q are available to serve these required arcs. Initially, all vehicles are stationed at the central depot from which each vehicle starts a single route at a certain vehicle departure time. The route starts and ends in the depot. For the sake of convenience, the depot is used as a dummy required arc (task), represented by the unique ID 0. The value of each attribute of the depot is set to 0, such as service cost, service time and demand, etc. Notably, since no waiting time is permitted on the route, the arrival time of the task is equal to its time of beginning of service. The objective is to get a feasible solution with minimum total cost. In [8] [9], it is noted that in winter gritting applications, if the vehicle departure time is different, the cost in time will be different. Consequently, in this context, the total cost incurred is specified as the total time expended, which means that the service cost and the travel cost are equal to the service time and the travel time, respectively. Therefore, in this paper, the time-dependent service cost is actually the time-dependent service time. The mathematical form of the objective function is as follows:

$$\min C(X, T) = \sum_{k=1}^m C(R_k, t_k), \quad (1)$$

where have two types of decision variables, denoted as X and T , representing the routing plan and the vehicle departure time, respectively. Therefore, the feasible solution S consists of two

parts, i.e., X and T , which can be expressed as $S = (X, T)$. Specifically, $X = (R_1, R_2, \dots, R_m)$ and $T = (t_1, t_2, \dots, t_m)$, where m indicates the number of routes or vehicles. Each R_k represents the route served and traveled by vehicle k , expressed as $R_k = (re_0^k, re_1^k, re_2^k, \dots, re_{l_k}^k, re_{l_k+1}^k)$. In essence, R_k comprises depot 0, required arcs $(re_1^k, re_2^k, \dots, re_{l_k}^k)$ and travel arcs $(de_1^k, de_2^k, \dots, de_{p_k}^k)$. These travel arcs result from the shortest paths between every two neighboring (dummy) required arcs in the route. The shortest paths are gotten through Dijkstra's algorithm [13]. Fig. 1 presents a simple illustration of the routing plan representation. The routing plan $X = (0, 1, 3, 0, 2, 4, 0)$. In X , 0 is the separator, denoting the depot. And each $r \in (1, 3, 2, 4)$ represents a task. Notably, every sequence of tasks enclosed by two separators (including separator 0) represents a route. So X comprises two routes, i.e., $(0, 1, 3, 0)$ and $(0, 2, 4, 0)$.

Additionally, $C(R_k, t_k)$ denotes the cost of the route R_k at vehicle departure time t_k , with a mathematical formula as follows:

$$C(R_k, t_k) = \sum_{i=1}^{l_k} SC(re_i^k, T_{re_i^k}(t_k)) + \sum_{i=1}^{p_k} DC_{de_i^k}, \quad (2)$$

where l_k and p_k represent the numbers of the required arcs (except the dummy required arc, i.e., depot) and the travel arcs in the route R_k , respectively, and $k \in \{1, 2, \dots, m\}$. $SC(re_i^k, T_{re_i^k}(t_k))$ denotes the service cost of the required arc re_i^k with its time of beginning of service $T_{re_i^k}(t_k)$, where $i \in \{1, 2, \dots, l_k\}$. $T_{re_i^k}(t_k)$ can be further expressed as $T_{re_i^k}(t_k) = t_k + \sum_{h=0}^{i-1} st_{re_h^k} + \sum_{h=0}^{i-1} dt_{sp_h^k}$, where $st_{re_h^k}$ denotes the service time of the h -th required arc and $dt_{sp_h^k}$ is the travel time of the shortest path sp_h between the h -th and $(h+1)$ -th required arcs and $h \in \{0, 1, \dots, i-1\}$. Additionally, $DC_{de_i^k}$ represents the travel cost of the travel arc de_i^k , where $i \in \{1, 2, \dots, p_k\}$.

In addition to the objective function, CARPTDSC has some constraints whose mathematical formulas are as follows.

$$re_0^k = re_{l_k+1}^k = 0, \quad (3)$$

$$re_i^k \neq re_{i'}^{k'}, \forall (k, i) \neq (k', i'), \quad (4)$$

$$re_i^k \neq inv(re_{i'}^{k'}), \forall (k, i) \neq (k', i'), \quad (5)$$

$$\sum_{k=1}^m l_k = |A_1|, \quad (6)$$

$$\sum_{i=1}^{l_k} d(re_i^k) < Q, \quad (7)$$

$$0 \leq T_{re_i^k}(t_k) \leq T. \quad (8)$$

In the Eqs. (3)-(8), $k \in \{1, 2, \dots, m\}$. In the Eqs. (4)-(5), $i \in \{1, 2, \dots, l_k\}$, and $i \in \{0, 1, \dots, l_k, l_k+1\}$ in the Eq. (8). Eq. (3) represents the constraint that each route must begin and end at the depot. Eqs. (4)-(6) denote the constraint that each required arc can be served only once. In Eq. (5), $inv(re_{i'}^{k'})$ represents the arc $re_{i'}^{k'}$ with the reverse direction of itself (if $inv(re_{i'}^{k'})$ exists). $|A_1|$ in Eq. (6) denotes the number of all required arcs in the set of required arcs A_1 . Eq. (7) is the capacity constraint

which means that the total demand of each route doesn't exceed the capacity of the vehicle. The last constraint is the time constraint, as shown in Eq. (8), which indicates that the time of beginning of service on each (dummy) required arc must be within the planning horizon $[0, T]$.

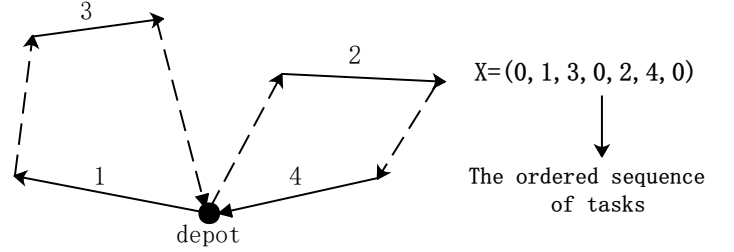


Figure 1: Illustration of the routing plan representation. Each solid line and each dotted line represent a required arc (task) and a travel arc, respectively.

2.2. MAENS

MAENS [2] is a state-of-the-art method for solving static CARP. It includes initialization, crossover, three local search operators, and a novel large-neighborhood operator. This section mainly details the initialization strategy of MAENS.

2.2.1. Initialization strategy of MAENS

The initialization strategy in MAENS is to generate the initial population with p_{size} distinct individuals. This process of generating an individual is termed individual initialization strategy here, whose main purpose is to generate an initial routing plan that contains all tasks.

The individual initialization strategy is a constructive heuristic strategy, and its process of constructing the routing plan is the process of constructing routes one by one. When constructing a route, the route is first initialized to empty, and then 0 (i.e., depot) is added to the route. Then one task is added iteratively to the route. When selecting the task to be added, the task nearest to the end of the current route (i.e., the head node of the last task) is selected from all the unserved and feasible tasks. If multiple tasks meet the selection condition at the same time, the tie-breaking rule selected at this time is to randomly select one from multiple tasks that meet the condition. When there is no feasible task to select, 0 is added to the route. At this time, the process of constructing a route ends.

2.3. Related work

In [14], CARP was introduced for the first time, and it was proved that CARP is NP-hard. Due to the limitations of exact algorithms in handling only small-scale instances, the research community has increasingly embraced heuristic and meta-heuristic approaches. Prominent heuristic algorithms include construct-strike [15], path-scanning [16], and augment-merge [14]. And many meta-heuristic methods are also applied, including tabu search [17], variable neighborhood descent [18], guided local search [19], evolutionary algorithm [3, 20], memetic algorithm (or hybrid genetic algorithm) [2, 21, 22].

Compared to ARP, vehicle routing problem (VRP) or node routing problem is a more extensively studied routing problem, commonly applied in logistics. Due to the extensive research on VRP, some ARPs are transformed into VRPs for resolution [23, 24], including CARPTDSC [8]. And among various VRPs, TDVRP is the one that has the same kind of characteristics as the time-dependent arc routing problem (TDARP), i.e., time-dependent. Therefore, understanding the solving algorithms for TDVPR is also very helpful to address TDARPs. In TDVRP, the travel time is generally time-dependent, influenced by factors such as the distance between two customers and the time of day. Numerous TDVRPs have been formulated as mixed integer programming models [25, 26]. Algorithms for dealing with TDVRP include exact algorithms, heuristic algorithms, and meta-heuristic algorithms. Among them, the exact algorithms include branch-and-price method [27] and dynamic programming [28, 29]. The heuristic algorithm has mathematical-programming-based heuristic [25]. Additionally, meta-heuristic algorithms encompass genetic algorithm [30], and ant colony algorithm [31, 32].

Although some ARPs can be transformed into VRPs for resolution, it is advantageous to design algorithms specifically for ARPs. In the original form of the problem, it is easier to exploit the characteristics of the problem [10]. In addition, the transformation from VRP to ARP increases the dimension of the problem and reduces the attempt to use the VRP algorithms to solve ARP [33]. Regarding TDARPs, some algorithms have been designed. Sun et al. [34] proposed a new integer programming formulation for the Chinese postman problem with time-dependent travel times, which significantly reduces the size of the circuit formulation. Black et al. [35] studied a time-dependent prize-collecting arc routing problem in which travel time changes with the time of day. Then, two metaheuristic algorithms were proposed to address this problem. Nossack et al. [36] proposed the windy rural postman problem with a time-dependent zigzag option, which was modeled as (mixed) integer programming formulation and then an exact algorithm was used to solve the problem. Calogiuri et al. [37] mainly dealt with the time-dependent rural postman problem where the travel time of certain arcs varies in the planning horizon. Branch-and-bound algorithm was developed to solve this problem.

Jin et al. [1] studied a capacitated arc routing problem with time-dependent penalty costs, which stems from the planning of garbage collection services. Penalty costs are related to parking patterns and service periods. The problem was formalized as a mixed integer linear model and a problem-specific intelligent heuristic search approach was proposed for its resolution. Ahabchane et al. [38] dealt with the mixed capacitated general routing problem with time-dependent demands. CPLEX was used to solve small-scale instances and slack induction by string removals metaheuristic method was developed to address large-scale instances. Additionally, Vidal et al. [39] studied a capacitated arc routing problem with time-dependent travel times and paths, marking the first exploration of CARP with time-dependent travel times at the network level. Branch-and-price algorithm and hybrid genetic search were proposed for

solving such problems.

Algorithm 1: The general framework of MAENS-GN

Input: A TDCARP instance $inst$;
Output: The routing plan X_{bf} and the vehicle departure time Dt ;

- 1 Get the routing plan X_{bf} by MAENS($inst$);
- 2 Get the instance type $intp$ from $inst$;
// Based on the analyzed relationship between the route cost and vehicle departure time under various scenarios (2LP, 3LP (slope $|k| \leq 1$ and $|k| > 1$)), vehicle departure time begins to be optimized.
- 3 **if** $intp == 2LP$ **then**
- 4 $n \leftarrow$ the number of routes in X_{bf} ;
- 5 **for** $i \leftarrow 1 : n$ **do**
- 6 $Dt \leftarrow Dt \cup 0$;
- 7 **end**
- 8 **end**
- 9 **else if** $intp == 3LP$ **then**
- 10 **if** $|k| \leq 1$ **then**
- 11 $Dt \leftarrow GSS(X_{bf}, \mathbf{0}, T)$;
- 12 **end**
- 13 **else if** $|k| > 1$ **then**
- 14 $Dt \leftarrow NCS(X_{bf}, \mathbf{0}, T)$;
- 15 **end**
- 16 **end**
- 17 **return** X_{bf} and Dt

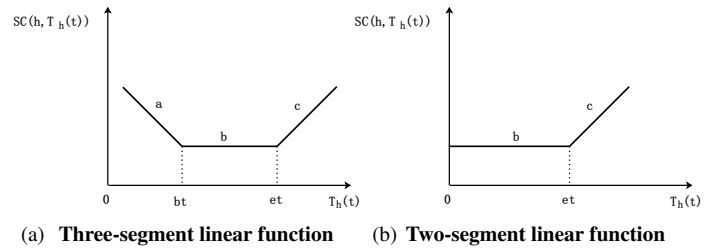


Figure 2: Schematic diagram of two types of linear functions between the service cost of task h and its time of beginning of service. a , b , and c represent the decreasing, unchanged, and increasing segments, respectively.

Despite several studies on various types of TDARPs, limited research has been dedicated solely to CARPTDSC. Tagmouti et al. [8] first introduced time-dependent service costs to CARP which originates from winter gritting applications. Since the relationship between the service cost of each task and its time of beginning of service was modeled as a three-segment linear function, the type of CARPTDSC is 3LP. This problem was initially transformed into a node routing problem and addressed through a column generation approach. However, the exact algorithm can only address the small-scale instances in which the number of tasks is only up to 40. To tackle larger-scale instances, Tagmouti et al. [9] proposed a variable neighborhood

descent heuristic (VND). For simplicity, a two-segment linear function was employed to represent the relationship between the service cost of the task and its time of beginning of service, which is a degenerate form of three-segment linear function. Therefore, the type of CARPTDSC is 2LP, in which the route has the lowest cost if the corresponding vehicle starts service from time 0. In this case, the need for further departure time determination is eliminated and the problem's complexity is reduced. What's more, VND was less effective, which fails to reach optimal solutions in all test instances. To incorporate more practical considerations, Tagmouti et al. [10] introduced a dynamic factor to CARPTDSC, i.e., changes in the optimal service time interval due to updates from weather forecasts. An adapted VND was used to address this problem. In the above papers [8–10], it is mentioned that the cost in time is time-dependent. However, the service time of the task is still assumed to be constant. Therefore, this is a bit unrealistic.

3. The proposed dual-stage algorithm

The proposed dual-stage algorithm is termed MAENS-GN, which is divided into two stages, i.e., the routing stage and the vehicle departure time optimization stage. The general framework is described in Algorithm 1. In the routing stage, MAENS [2] was used to get the routing plan, i.e., X_{bf} (line 1). When using MAENS to get X_{bf} , the evaluations need to be modified into time-dependent evaluations, which will not be described here. Furthermore, the initialization strategy of MAENS has been adapted to novel initialization strategy. After X_{bf} is obtained, the vehicle departure time Dt begins to be optimized based on the analyzed relationship between the route cost and the vehicle departure time under various scenarios in the vehicle departure time optimization stage. If the problem is 2LP, time 0 is the optimal vehicle departure time (lines 3-8). If the problem is 3LP, suitable methods are employed to search the (approximately) optimal departure time from the planning horizon $[0, T]$ according to the absolute value (i.e., $|k|$) of the slope (lines 9-16). MAENS-GN introduces two key innovations: the optimization of vehicle departure time and the novel initialization strategy. The subsequent sections provide a detailed description of these two components.

3.1. Optimization of the vehicle departure time

This optimization of the vehicle departure time is divided into two parts below, namely, the analysis of the relationship between the route cost and the vehicle departure time, and the methods for optimizing the vehicle departure time.

3.1.1. Detailed analysis of the relationship between the route cost and the vehicle departure time

When analyzing the relationship between the route cost and the vehicle departure time, the travel cost is not calculated because it has no relationship with the vehicle departure time. It is worth noting that in this paper, the time-dependent service cost is specified for the time-dependent service time. We performed a detailed analysis of the relationship between the route

cost and the vehicle departure time for both the 2LP and 3LP (slope $|k| < 1$ and $|k| > 1$) scenarios. Since the relationship under $|k| = 1$ in the 3LP is similar to that under the $|k| < 1$, it will not be analyzed here. For convenience, in the 3LP, it is assumed that the absolute values of the slopes of three-segment linear functions of all tasks in an instance are the same, as done in [8]. For example, the absolute value of the slope is 2, which means the slopes of all tasks are 2 and -2, as shown in Fig. 3.

3.1.1.1. Detailed analysis of the relationship between the route cost and the vehicle departure time in the 2LP

1. When there is only one task, i.e., h , in the route, the relationship between the route cost and the vehicle departure time is consistent with the non-decreasing two-segment linear function of the task, as illustrated in Fig. 2(b).

2. When there are multiple tasks in the route, the service cost of each task has a non-decreasing relationship with its time of beginning of service. As the vehicle departure time increases, the time of beginning of service of each task will also increase. Consequently, the service cost of each task will also be non-increasing. The route cost is equal to the sum of the service costs of all tasks in the route. Therefore, the route cost will have a non-decreasing relationship with the vehicle departure time, as shown in Fig. 4(b).

Hence, whether there are one or more tasks in a route, the route cost has a non-decreasing relationship with the vehicle departure time. Consequently, time 0 is the optimal vehicle departure time for this route in the 2LP. This is also the reason why in [9], the algorithm does not need to solve for the vehicle departure time.

3.1.1.2. Detailed analysis of the relationship between route cost and vehicle departure time in the 3LP with the slope $|k| < 1$.

When $|k| < 1$ in the 3LP, the analysis needs to be divided into two stages. Firstly, it is necessary to analyze the relationship between the time of beginning of service of each task in the route and the vehicle departure time. Secondly, the relationship between the route cost and the vehicle departure time is analyzed. In the first stage, it has been observed that as the vehicle departure time increases, the time of beginning of service of each task in the route also increases. The main analysis process is as follows.

Assume that there are n tasks in the route. When the vehicle departure time dt increases by Δt (Δt is a sufficiently small positive real number), if the increase of time of beginning of service of the i -th ($1 \leq i \leq n$) task in the route is to be minimal, the time of beginning of service of the tasks before i -th task in the route need to be in the decreasing segments (i.e., segment a in Fig. 2(a)). In this case, when dt increases by Δt , the time of beginning of service of the first task increases by Δt , and its service time (i.e., service cost) will decrease by $|k|\Delta t$. Consequently, the time of beginning of service of the second task increases by $(1 - |k|)\Delta t$, and its service time will decrease by $|k|(1 - |k|)\Delta t$. Therefore, the time of beginning of service of the third task will increase by $(1 - |k|)^2\Delta t$. It can be deduced that the time of beginning of service of the i -th task will increase by $(1 - |k|)^{i-1}\Delta t$. Because $|k| < 1$, $0 < (1 - |k|) < 1$. Therefore, among all the

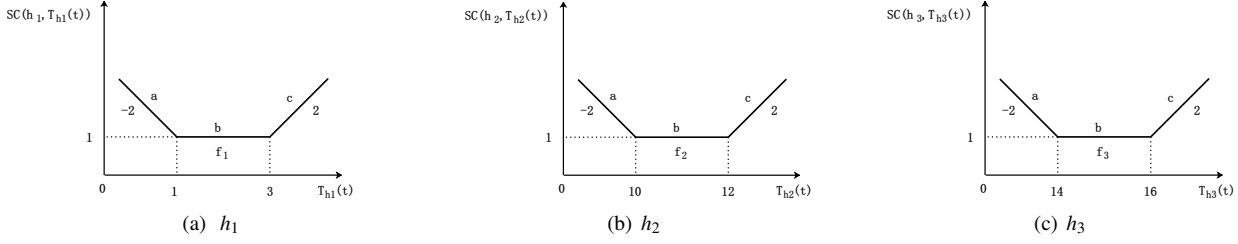


Figure 3: Three-segment linear functions of the service cost of the three tasks (h_1 , h_2 and h_3) in the route and their time of beginning of service.

tasks in the route, the last task (i.e., the n -th task) experiences the least increase in time of beginning of service, which increases by $(1 - |k|)^{n-1} \Delta t$. This value is still positive. Why is it that when the time of beginning of service of the tasks before n -th task in the route is all within the decreasing segments, the increase of the time of beginning of service of the n -th task is minimal as dt increases by Δt ? Below is an example. Among the n tasks in the route, the time of beginning of service of only the i -th ($i < n$) task is not within the decreasing segment, but within the increasing segment (i.e., segment c in Fig. 2(a)). At this time, the time of beginning of service of the n -th task is $(1 + |k|)(1 - |k|)^{n-2}$, which is greater than $(1 - |k|)^{n-1}$. Therefore, as dt increases, the time of beginning of service of each task in the route also increases. The analysis of the second stage is as follows.

When dt is 0, the time of beginning of service of the tasks in the route lies within different segments (e.g., segments a , b , or c in Fig. 2(a)) of the three-segment linear functions. Therefore, when dt increases by Δt from 0 (i.e., $dt = \Delta t$), the service costs of the tasks in the route may be decreasing, unchanged, or increasing. Assume that the change of the route cost at this time is tc_0 . As dt continues to increase with the size of Δt , the time of beginning of service of all tasks in the route will also continue to increase, gradually approaching the increasing segment (i.e., segment c in Fig. 2(a)) or continuing to increase in the increasing segment. In the end, the time of beginning of service of all tasks will fall within the increasing segment. Consequently, if $tc_0 < 0$, as dt increases continually, the change in route cost will gradually become greater than 0. During this period, the route cost will initially decrease (then remain unchanged), and finally increase, showing a (similar) unimodal trend as shown in Fig. 4(a). Conversely, if $tc_0 \geq 0$, with the continued increase of dt , the relationship between the route cost and the vehicle departure time will show a non-decreasing trend, as shown in Fig. 4(b).

Therefore, in the 3LP with slope $|k| < 1$, the relationship between the route cost and the vehicle departure time exhibits a (similar) unimodal or non-decreasing trend.

3.1.1.3. Detailed analysis of the relationship between route cost and vehicle departure time in the 3LP with slope $|k| > 1$.

When $|k| > 1$, the relationship between the route cost and the vehicle departure time no longer meets the (similar) unimodal property. This is mainly because when dt increases by Δt , the time of beginning of service of the task in the route may not increase, but appears to decrease. An illustrative example is

provided below.

A route contains three tasks (i.e., h_1 , h_2 , h_3), and their three-segment linear functions (i.e., f_1 , f_2 , f_3) are shown in Fig. 3, and the absolute value of the slopes is 2. The ranges of segments b of f_1 , f_2 , and f_3 are $[1, 3]$, $[10, 12]$ and $[14, 16]$, respectively. Among the three functions, the minimum service costs of the tasks are 1. The route can be represented by the sequence of tasks $h_1 h_2 h_3$, with the depot positioned at the tail node of h_1 and the head node of h_3 . The three tasks are directly connected, signifying that the head node of h_1 is equal to the tail node of h_2 , and the head node of h_2 is equal to the tail node of h_3 . Let $T_h(dt)$ (where $h \in \{h_1, h_2, h_3\}$) represents the time to arrive at task h , and $SC(h, T_h(dt))$ represents the service cost of task h at $T_h(dt)$. Assume that the time Δt by which dt increases each time is 1.

When $dt = 0$, $T_{h_1}(dt = 0) = 0$. At this time, according to f_1 , $SC(h_1, 0) = (1 - 0) * 2 + 1 = 3$. And $T_{h_2}(0) = SC(h_1, 0) + T_{h_1}(0) = 3$. According to f_2 , $SC(h_2, 3) = 15$. And $T_{h_3}(0) = T_{h_2}(0) + SC(h_2, 3) = 18$. According to f_3 , $SC(h_3, 18) = 5$. Let $tc(x)$ represent the sum of service costs of all tasks in the sequence of tasks x . Therefore, $tc(h_1 h_2) = SC(h_1, 0) + SC(h_2, 3) = 18$, and $tc(h_1 h_2 h_3) = SC(h_1, 0) + SC(h_2, 3) + SC(h_3, 18) = 23$.

When dt increases by Δt , $dt = 1$. At this moment, $T_{h_2}(1) = 2$ and $tc(h_1 h_2 h_3) = 25$. When $dt = 2$, $T_{h_2}(2) = 3$, and $tc(h_1 h_2 h_3) = 21$. Furthermore, when $dt = 10$, $T_{h_2}(10) = 25$ and $tc(h_1 h_2 h_3) = 115$.

From the above computations, it is evident that when dt is 0, 1, 2, and 10 respectively, $T_{h_2}(dt)$ is 3, 2, 3, and 25, respectively. The route cost, i.e., $tc(h_1 h_2 h_3)$, are 23, 25, 21, 115 respectively. It can be observed that as dt increases from 0 to 1, $T_{h_2}(dt)$ decreases from 3 to 2. At the same time, as dt increases continually from 0, the route cost initially increases, then decreases, and subsequently increases again, which demonstrates a non-unimodal relationship, as shown in Fig. 4(c).

3.1.2. Methods for optimizing the vehicle departure time

In the 2LP, time 0 is the optimal vehicle departure time.

In the 3LP, when the slope $|k| \leq 1$, the route cost and the departure time of the vehicle exhibit a (similar) unimodal or non-decreasing relationship. In this case, GSS [11] is used to quickly identify the optimal vehicle departure time for each route in the routing plan. GSS, characterized as an interval search method, initiates with the entire planning horizon, i.e., $[0, T]$, and successively narrows down the search interval using the golden ratio until the length of the search interval becomes

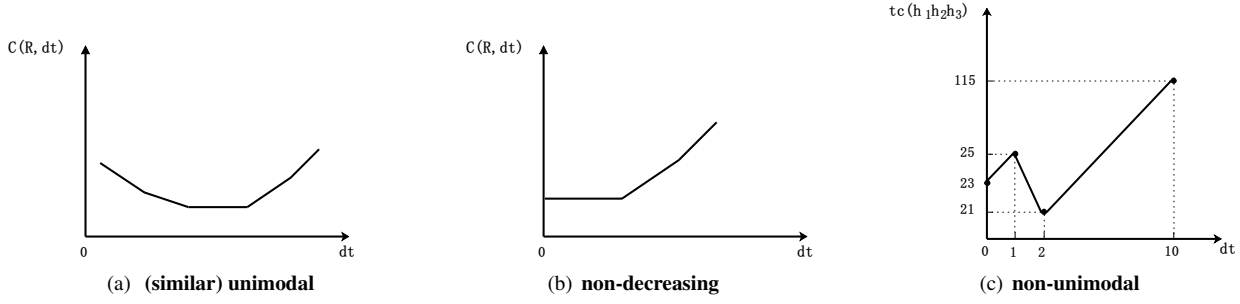


Figure 4: Schematic diagram of the relationship between the route cost $C(R, dt)$ or $tc(h_1h_2h_3)$ and vehicle departure time dt .

Table 1: Results on the *gdb* benchmark test set in the 2LP in terms of costs of solutions. For each instance, the average performance of an algorithm is indicated in bold if it is the best among all comparison algorithms. “ \ddagger ” and “ \dagger ” indicate MAENS-GN performs significantly better than and equivalently to the corresponding algorithm based on 20 independent runs according to the Wilcoxon rank-sum test with significant level $p = 0.05$, respectively.

Instances	R	LB	MAENS-GN			VND			VND*	
			Ave(std)	Best	Time	Ave(std)	Best	Time	Ave(std)	Best
<i>gdb1</i>	22	316	316.0(0.00)	316	0.799	363.0(0.00) \ddagger	363	0.102	359.5(5.82) \ddagger	340
<i>gdb2</i>	26	339	345.2(0.65)	345	8.505	379.6(2.82) \ddagger	375	0.149	372.4(9.30) \ddagger	346
<i>gdb3</i>	22	275	289.0(0.00)	289	6.131	315.4(0.49) \ddagger	315	0.088	307.7(8.25) \ddagger	289
<i>gdb4</i>	19	287	287.0(0.00)	287	1.118	342.0(0.00) \ddagger	342	0.056	334.9(7.65) \ddagger	317
<i>gdb5</i>	26	377	381.7(3.84)	377	7.287	417.0(0.00) \ddagger	417	0.121	407.4(9.83) \ddagger	388
<i>gdb6</i>	22	298	299.3(5.67)	298	1.395	344.0(0.00) \ddagger	344	0.085	339.2(7.65) \ddagger	324
<i>gdb7</i>	22	325	325.0(0.00)	325	1.548	377.8(4.28) \ddagger	364	0.088	359.0(13.57) \ddagger	335
<i>gdb8</i>	46	348	357.1(1.48)	355	34.872	395.0(0.00) \ddagger	395	0.588	389.8(5.78) \ddagger	370
<i>gdb9</i>	51	303	312.0(3.19)	309	38.796	358.2(4.59) \ddagger	346	0.836	343.2(4.36) \ddagger	336
<i>gdb10</i>	25	275	278.6(4.04)	275	5.327	313.8(5.08) \ddagger	309	0.117	306.6(7.45) \ddagger	290
<i>gdb11</i>	45	395	403.8(2.14)	399	32.816	446.1(2.86) \ddagger	435	0.671	429.8(4.36) \ddagger	421
<i>gdb12</i>	23	458	458.0(0.00)	458	1.061	503.0(0.00) \ddagger	503	0.082	503.0(0.00) \ddagger	503
<i>gdb13</i>	28	536	545.4(4.75)	536	9.129	586.0(6.49) \ddagger	578	0.150	569.7(4.52) \ddagger	560
<i>gdb14</i>	21	100	101.5(1.50)	100	4.179	109.0(0.00) \ddagger	109	0.072	107.0(1.73) \ddagger	104
<i>gdb15</i>	21	58	58.0(0.00)	58	0.255	62.0(0.00) \ddagger	62	0.072	61.5(1.07) \ddagger	58
<i>gdb16</i>	28	127	129.0(0.00)	129	10.749	137.0(0.00) \ddagger	137	0.146	133.1(1.04) \ddagger	131
<i>gdb17</i>	28	91	91.0(0.00)	91	0.123	92.4(0.92) \ddagger	91	0.161	92.8(0.60) \ddagger	91
<i>gdb18</i>	36	164	169.4(1.56)	164	14.403	178.2(3.18) \ddagger	172	0.307	173.2(1.44) \ddagger	171
<i>gdb19</i>	11	55	55.0(0.00)	55	0.053	63.0(0.00) \ddagger	63	0.020	62.1(1.84) \ddagger	55
<i>gdb20</i>	22	121	122.8(0.60)	121	6.309	125.0(0.00) \ddagger	125	0.070	124.8(0.51) \ddagger	123
<i>gdb21</i>	33	156	157.9(0.54)	156	12.504	169.2(2.17) \ddagger	166	0.236	165.4(2.15) \ddagger	162
<i>gdb22</i>	44	200	202.2(0.60)	202	25.411	206.0(0.00) \ddagger	206	0.538	205.2(1.01) \ddagger	203
<i>gdb23</i>	55	233	237.5(0.92)	236	41.476	244.0(0.00) \ddagger	244	1.003	243.8(0.36) \ddagger	243
w-d-1	-	-	-	-	-	23-0-0	-	-	23-0-0	-
No.best	-	-	9	23	-	0	1	-	0	4
Ave.PDR	-	-	1.37%	-	-	10.82%	-	-	8.74%	-
Ave.Time	-	-	-	-	11.489	-	-	0.25	-	-

smaller than a threshold ε . At this point, the optimal vehicle departure time is determined. In addition, GSS is an algorithm with low time complexity. For more details on GSS, please refer to [11].

In the 3LP, when the slope $|k| > 1$, the route cost and the departure time of the vehicle exhibit a non-unimodal relationship, and GSS is no longer applicable. In such a scenario, an evolutionary algorithm, that is, NCS [12], is employed to obtain the (approximately) optimal vehicle departure time. NCS is good at dealing with complex optimization problems. It mainly maintains the search process of multiple individuals in parallel, and models the individual search process as a probability distribu-

tion. For more details on NCS, please refer to [12].

3.2. Novel initialization strategy

When constructing a route in the individual initialization strategy of MAENS, the nearest task to the end of the route needs to be selected to add to the route. If more than one task satisfies the condition simultaneously, these tasks form a task set termed $Tasks_{nearst}$. At this time, the tie-breaking rule selected is to randomly select one from $Tasks_{nearst}$. However, this stochastic tie-breaking rule is a little blind in the CARPTDSC. Because in the CARPTDSC, the service cost of the task is time-dependent, meaning that the task’s service cost varies based on

Table 2: Results on the *egl* benchmark test set in the 2LP in terms of costs of solutions. For each instance, the average performance of an algorithm is indicated in bold if it is the best among all comparison algorithms. “‡” and “†” indicate MAENS-GN performs significantly better than and equivalently to the corresponding algorithm based on 20 independent runs according to the Wilcoxon rank-sum test with significant level $p = 0.05$, respectively.

Instances	R	LB	MAENS-GN			VND			VND*	
			Ave(std)	Best	Time	Ave(std)	Best	Time	Ave(std)	Best
egl-e1-A	51	3548	3550.6(8.97)	3548	28.973	4323.8(110.19)‡	4018	0.687	4033.2(94.85)‡	3900
egl-e1-B	51	4498	4576.9(18.31)	4557	74.811	5006.6(35.66)‡	4877	0.902	4760.1(80.10)‡	4573
egl-e1-C	51	5595	5677.6(59.91)	5595	66.548	6178.4(71.04)‡	5923	1.017	6091.4(84.25)‡	5907
egl-e2-A	72	5018	5102.4(64.53)	5018	189.315	5886.0(158.29)‡	5558	2.552	5425.3(73.00)‡	5307
egl-e2-B	72	6317	6424.9(26.91)	6355	163.441	7114.4(75.27)‡	6869	1.765	6703.0(66.97)‡	6554
egl-e2-C	72	8335	8599.0(64.46)	8474	163.261	8910.6(5.88)‡	8885	1.768	8779.8(101.86)‡	8548
egl-e3-A	87	5898	6099.4(77.63)	6002	335.078	6483.0(0.00)‡	6483	3.104	6475.2(34.00)‡	6327
egl-e3-B	87	7744	8040.6(71.43)	7909	251.941	8819.0(0.00)‡	8819	4.752	8491.9(94.51)‡	8264
egl-e3-C	87	10244	10460.6(54.10)	10390	213.761	11485.4(185.13)‡	10865	2.642	10928.1(141.76)‡	10429
egl-e4-A	98	6408	6710.6(100.79)	6580	364.345	7526.5(19.66)‡	7460	6.271	7222.0(81.88)‡	7075
egl-e4-B	98	8935	9329.9(78.16)	9165	318.551	10251.3(170.85)‡	9876	5.741	9748.6(101.41)‡	9438
egl-e4-C	98	11512	11992.6(91.87)	11854	264.948	12614.8(14.17)‡	12553	5.560	12484.6(114.52)‡	12225
egl-s1-A	75	5018	5145.9(102.02)	5018	218.771	5804.3(7.41)‡	5772	2.148	5613.8(154.15)‡	5267
egl-s1-B	75	6388	6576.6(106.89)	6394	187.171	6856.0(0.00)‡	6856	2.677	6856.0(0.00)‡	6856
egl-s1-C	75	8518	8783.8(62.16)	8677	162.748	9643.8(17.13)‡	9573	2.794	9479.2(96.17)‡	9256
egl-s2-A	147	9825	10490.1(60.67)	10392	1172.03	11414.2(86.52)‡	11037	23.580	11204.4(109.18)‡	11015
egl-s2-B	147	13017	13887.2(119.45)	13698	795.669	14680.0(0.00)‡	14680	14.923	14661.8(30.65)‡	14567
egl-s2-C	147	16425	17392.6(139.47)	17165	761.257	18408.6(14.82)‡	18344	18.951	18327.3(83.45)‡	18174
egl-s3-A	159	10165	10733.0(99.71)	10593	1417.264	11764.7(75.41)‡	11436	19.466	11406.1(100.94)‡	11207
egl-s3-B	159	13648	14418.0(125.53)	14168	1046.018	15858.4(169.85)‡	15367	27.001	15325.0(93.46)‡	15111
egl-s3-C	159	17188	18269.3(151.44)	17983	902.040	19666.0(0.00)‡	19666	22.921	19277.8(155.11)‡	19029
egl-s4-A	190	12153	13197.1(152.21)	12932	1531.802	14918.2(319.64)‡	14285	46.072	14142.2(139.63)‡	13762
egl-s4-B	190	16113	17260.1(91.44)	17121	1499.895	18407.2(12.20)‡	18354	34.835	18242.6(144.89)‡	17943
egl-s4-C	190	20430	21796.0(188.09)	21427	1348.113	22996.4(2.83)‡	22984	37.787	22945.9(113.44)‡	22513
w-d-1	-	-	-	-	-	24-0-0	-	-	24-0-0	-
No.best	-	-	0	24	-	0	0	-	0	0
Ave.PDR	-	-	4.18%	-	-	13.80%	-	-	10.48%	-
Ave.Time	-	-	-	-	561.573	-	-	12.08	-	-

its position (i.e., the time of beginning of service) in the route. Consequently, this stochastic tie-breaking rule may select a task with the larger service cost caused by its time of beginning of service being distant from its optimal service time interval, such as the time of beginning of service of h_1 is 10 in Fig. 3(a).

In this context, we design a specialized tie-breaking rule that takes into account the time-dependent property of CARPTDSC in the individual initialization strategy. If choosing the task with the smallest service cost from $Tasks_{nearst}$, the time of beginning of service of the selected task may fall within or not far from its optimal service time interval (e.g., the time interval $[bt, et]$ in Fig. 2(a)). In this way, it is avoided that the task is in another position (i.e., the time of beginning of service of the task is far away from its optimal service time interval) of the route, resulting in a larger service cost. Because each task needs to be inserted into the routing plan and only once, selecting the task being in a good position can avoid the increase of service cost caused by its being in a bad position. In this way, the further increase of the route cost is avoided. However, if doing this, the individuals produced in the initial population will all be the same, meaning no diversity. So this is not a good method. To address this, we devised a roulette wheel selection-based [40] approach where the task with the smaller service cost will have a greater probability of being selected. Therefore, this method

not only considers diversity but also makes tasks with better quality more likely to be selected.

Here we will select a task from $Tasks_{nearst}$ by the roulette wheel selection strategy and one score is associated with each task in $Tasks_{nearst}$. The higher the score of the task, the higher the probability of being selected. Due to the need to make the service cost of the task lower, the probability of being selected is higher. Consequently, we define the score of task x , denoted as $score(x)$, to be equal to the reciprocal of the task’s time-dependent service cost, as expressed in Eq. (9).

$$score(x) = \frac{1}{SC(x, t)}, \quad (9)$$

where $SC(x, t)$ is the time-dependent service cost of task x . The probability of the task x_i being selected, denoted as $p(x_i)$, is the proportion of the score of task x_i to the sum of the scores of all tasks in $tasks_{nearst}$, as shown in Eq. (10).

$$p(x_i) = \frac{score(x_i)}{\sum_{j=1}^N score(x_j)}, \quad (10)$$

where N is the size of $Tasks_{nearst}$. The detailed process of the roulette wheel selection will not be introduced in detail below. For more details on roulette wheel selection, please refer to the [40]. Below is an illustrative example.

Table 3: Results on the *Solomon-25* benchmark test set in the 3LP in terms of costs of solutions. For each instance, the average performance of an algorithm is indicated in bold if it is the best among all comparison algorithms (except CG). “‡” and “†” indicate MAENS-GN performs significantly better than and equivalently to the corresponding algorithm based on 20 independent runs according to the Wilcoxon rank-sum test with significant level $p = 0.05$, respectively.

Instances	CG		MAENS-GN			VND-GN		
	Cost	Time	Ave(std)	Best	Time	Ave(std)	Best	Time
r101	893.7	258.4	1014.3(10.86)	1003.4	10.725	1089.9(34.49)‡	1050.3	0.100
r102	806.0	410.0	865.5(11.79)	853.8	9.955	908.1(3.68)‡	900.8	0.095
r103	726.1	80.5	770.7(2.14)	767.0	10.525	819.2(6.22)‡	806.8	0.095
r104	690.0	571.1	715.2(8.01)	703.0	6.865	767.8(27.37)‡	736.8	0.086
r105	780.4	118.2	839.7(3.18)	836.3	10.140	946.1(38.53)‡	853.9	0.090
r106	721.4	236.9	744.0(4.61)	740.1	9.595	864.6(7.33)‡	847.3	0.097
r107	679.5	137.8	700.5(2.81)	697.5	9.850	760.0(9.95)‡	740.1	0.092
r108	647.7	232.9	663.1(10.17)	653.1	6.900	712.0(17.36)‡	689.4	0.087
r109	691.3	71.7	744.0(2.33)	734.7	9.460	822.5(22.36)‡	777.8	0.087
r110	668.8	125.9	716.8(10.05)	697.2	15.925	758.8(23.82)‡	729.8	0.093
r111	676.3	157.8	710.5(5.16)	707.9	16.575	778.9(16.80)‡	746.3	0.094
r112	643.0	356.1	666.3(5.17)	656.0	15.925	718.3(13.18)‡	696.1	0.088
rc101	623.8	62.4	648.4(3.07)	643.9	19.290	761.3(58.66)‡	681.7	0.090
rc102	598.3	179.8	611.5(5.07)	606.6	20.185	803.9(36.15)‡	761.5	0.103
rc103	585.1	941.5	607.8(4.96)	598.1	20.005	738.2(26.23)‡	645.4	0.089
rc104	572.4	3183.1	603.3(3.52)	595.4	20.705	609.0(0.00)‡	609.0	0.077
rc105	623.1	743.7	656.3(9.24)	641.1	21.335	813.6(62.44)‡	677.3	0.082
rc106	588.7	372.6	605.6(0.00)	605.6	18.370	631.3(0.00)‡	631.3	0.084
rc107	548.3	824.8	567.0(2.15)	565.4	12.530	628.5(11.66)‡	600.1	0.079
rc108	544.5	3457.1	553.5(4.42)	546.8	12.630	579.7(13.99)‡	555.9	0.075
w-d-1	0-0-20	-	-	-	-	20-0-0	-	-
No.best	20	-	0	0	-	0	0	-
Ave.PDR	0.00%	-	4.95%	-	-	16.44%	-	-
Ave.Time	-	626.115	-	-	13.875	-	-	0.089

Assume that there are only two tasks h_2 and h_3 (in Fig. 3) that have not been inserted into the initial routing plan X_{init} , and both tasks are in $Tasks_{nearst}$, and the two tasks are connected directly. Therefore, the order of inserting into X_{init} of these two tasks depends on the task selected firstly from $Tasks_{nearst}$. Because the arrival time of the tasks in the $Tasks_{nearst}$ is the same, assume that it is 12. At this time, the service costs of h_2 and h_3 can be obtained to be $SC(h_2, 12) = 1$ and $SC(h_3, 12) = 5$, respectively. If roulette wheel selection is used, the probabilities of h_2 and h_3 being selected is $(1/1)/(1/1+1/5) \approx 0.83$ and 0.17, respectively. At this time, if h_2 is inserted firstly and then h_3 , then $SC(h_2, 12) = 1$ and $SC(h_3, 13) = 3$. The total cost of the sequence of tasks h_2h_3 is $tc(h_2h_3) = 1 + 3 = 4$. If h_3 is inserted firstly and then h_2 , then $SC(h_3, 12) = 5$ and $SC(h_2, 17) = 11$, leading to that a total cost of h_3h_2 is $tc(h_3h_2) = 16$. Using the roulette wheel selection, the probability of the total cost of the sequence h_2h_3 being 4 is 0.83, and the probability of the total cost of h_3h_2 being 16 is 0.17. In contrast, if the stochastic selection method is used, the probabilities of the total costs of the sequence of tasks being 4 and 16 would both be 0.5.

Therefore, the roulette wheel selection exhibits a higher likelihood of acquiring an initial solution with high quality.

4. Experimental studies

The experiments aim to verify whether MAENS-GN has effectively addressed the two research questions (RQ1 and RQ2).

Consequently, the verification of the performance of MAENS-GN is divided into two aspects.

1. In the 2LP, the quality of approximate solutions obtained by existing algorithms is not high, but does MAENS-GN significantly improve the quality of approximate solutions?
2. In the 3LP, the existing exact algorithms can only handle small-scale instances (number of tasks ≤ 40), whereas what is the quality of the solutions of MAENS-GN on larger-scale instances in addition to small-scale instances?

Additionally, we also assessed the contribution of the components in MAENS-GN, including GSS, NCS and the novel initialization strategy. In each instance, each algorithm was run independently 20 times to ensure robust evaluations.

4.1. Experimental setup

Two distinct types of benchmark test sets, i.e., test sets in the 2LP and 3LP, were utilized for evaluations. The *gdb* and *egl* in the 2LP, which already exist in [9], were modified based on the static test sets *gdb* [41] and *egl* [42], i.e., two-segment linear functions were added. In the 3LP, Solomon’s test set [43], as used in [8], was adopted. In [8], 25-customer, 35-customer, and 40-customer instances in Solomon’s test set were used, which are denoted as *Solomon-25*, *Solomon-35*, *Solomon-40* here. In addition to Solomon’s test set, the same method in [9] was used to apply the three-segment linear function on the static benchmark test set *gdb* and *egl*, making them time-dependent test sets

Table 4: Results on the *Solomon-35* benchmark test set in the 3LP in terms of costs of solutions. For each instance, the average performance of an algorithm is indicated in bold if it is the best among all comparison algorithms (except CG). “‡” and “†” indicate MAENS-GN performs significantly better than and equivalently to the corresponding algorithm based on 20 independent runs according to the Wilcoxon rank-sum test with significant level $p = 0.05$, respectively.

Instances	CG		MAENS-GN			VND-GN		
	Cost	Time	Ave(std)	Best	Time	Ave(std)	Best	Time
r101	1168.3	4165.8	1316.9(12.38)	1293.9	42.405	1373.4(6.25)‡	1369.5	0.312
r102	1048.0	6574.1	1097.3(7.34)	1085.0	45.620	1265.9(44.77)‡	1158.8	0.282
r103	929.2	5129.9	981.1(8.18)	969.4	43.460	1126.1(34.16)‡	1071.4	0.227
r104	837.8	6210.9	862.4(7.97)	853.4	49.230	921.9(9.63)‡	898.3	0.250
r105	1017.1	2926.2	1108.2(10.03)	1091.9	46.450	1186.5(17.82)‡	1156.7	0.300
r106	930.8	2247.1	968.5(9.10)	956.4	43.235	1090.6(27.85)‡	1045.2	0.277
r107	874.8	8957.4	911.8(10.55)	896.2	44.770	1011.2(21.72)‡	944.1	0.260
r108	805.7	14698.5	826.5(5.89)	820.3	47.030	887.7(28.64)‡	841.0	0.259
r109	914.8	8044.2	951.7(9.51)	942.0	43.595	1010.5(14.26)‡	976.1	0.274
r110	893.6	16259.7	910.5(8.71)	902.2	33.580	993.1(40.58)‡	948.5	0.257
r111	864.4	9957.6	895.6(5.86)	887.6	35.015	913.8(1.96)‡	907.2	0.290
r112	834.3	10377.9	839.6(2.84)	835.1	35.230	887.9(8.24)‡	854.3	0.239
w-d-1	0-0-12	-	-	-	-	12-0-0	-	-
No.best	12	-	0	0	-	0	0	-
Ave.PDR	0.00%	-	4.66%	-	-	13.58%	-	-
Ave.Time	-	7962.442	-	-	42.468	-	-	0.269

in the 3LP. In addition, a real-world *jd* dataset was also used, which is derived from the Jingdong logistics distribution system. The *jd* set is similar to Solomon’s test set, being also VRP test set with time windows. For convenience, the absolute values of the slopes in a instance of 3LP are the same, such as 2 and -2 in Fig. 3(a), as done in the [8]. The slope in the test sets in the 2LP is 1 [9]. The slopes in Solomon’s test set are 1 and -1 [8]. Furthermore, the absolute values of the slopes in the instances of other test sets, i.e., *gdb*, *egl*, and *jd* in the 3LP, were randomly chosen from the set {0.3, 0.5, 1, 2, 3}.

In the 2LP, the currently existing algorithm is variable neighborhood descent (VND) [9], which was as a comparison algorithm in solving 2LP. Because the vehicle departure time does not need to be calculated in the 2LP, MAENS-GN only needs to run the algorithm in the routing stage, i.e., MAENS. For a fairer comparison, VND* was added as a comparison algorithm, which denotes that VND runs the same time with MAENS-GN. During the time it takes MAENS-GN to complete one run, VND is run multiple times until it reaches the runtime of MAENS-GN and then stops, and finally the best value of the multiple values gotten by multiple runs is as the result of VND* running on that instance.

In the 3LP, the currently existing method is column generation (CG) [8], which serves as one comparison algorithm of MAENS-GN. The data that CG used in the comparative experiments were all provided by [8]. Because only Solomon’s test set is used in [8], CG only participated in the comparison of Solomon’s test set. Because the data [8] of CG on Solomon’s test set was obtained assuming that the service time remains unchanged. Therefore, when solving Solomon’s test set, for fairness, the evaluation functions of MAENS-GN need to be simply modified. But CG, being an exact algorithm, is limited to handling small-scale instances. To evaluate the performance of MAENS-GN on larger-scale instances, we adapted the algo-

rithm VND [9], which was initially designed for the 2LP. Since the primary difference between dealing with 2LP and 3LP is whether or not to optimize for vehicle departure time, the techniques for optimizing vehicle departure time (GSS and NCS) were incorporated into VND. VND-GN is formed in this way, which was as another comparison algorithm of MAENS-GN in the 3LP. For a fairer comparison, VND-GN* still acted as a comparison algorithm for MAENS-GN in the 3LP, just like VND* acting as a comparison algorithm for MAENS-GN in the 2LP. VND-GN* denotes that VND-GN runs the same time as MAENS-GN. What’s more, to verify the effects of GSS and NCS, MAENS and VND were also employed as comparison algorithms on the *gdb* and *egl* test sets in the 3LP. MAENS here denotes the method in the first stage of MAENS-GN.

In MAENS-GN, the population size (*psize*) was set to 10. The number of generations (*Gm*) was 50, and the probability of performing a local search (*Pls*) was 0.1. All other parameters in MAENS were consistent with those in [2]. In addition, the code for VND was reproduced from the description in [9]. There are two initialization methods in VND, i.e., the savings heuristic and the insertion heuristic, where the savings heuristic is a deterministic method. In the process of constructing a route in the insertion heuristic, each time one arc is required to be selected to insert into the current route. Among all candidate arcs, the next arc selected into the route is the arc that incurs the least additional cost to the route. However, in reality, there may be multiple arcs meeting this condition simultaneously, and the article [9] does not specify the tie-breaking rule. We opted for a stochastic tie-breaking rule, where an arc is randomly chosen from multiple arcs meeting the condition. Therefore, the insertion heuristic is a stochastic method, and VND is thus categorized as a stochastic algorithm. Because in [9], VND solves the CARPTDSC assuming constant service time. Therefore, the evaluation function of VND (or VND-GN) was

Table 5: Results on the *Solomon-40* benchmark test set in the 3LP in terms of costs of solutions. For each instance, the average performance of an algorithm is indicated in bold if it is the best among all comparison algorithms (except CG). “‡” and “†” indicate MAENS-GN performs significantly better than and equivalently to the corresponding algorithm based on 20 independent runs according to the Wilcoxon rank-sum test with significant level $p = 0.05$, respectively.

Instances	CG		MAENS-GN			VND-GN		
	Cost	Time	Ave(std)	Best	Time	Ave(std)	Best	Time
r101	1318.4	4467.3	1479.8(14.61)	1449.0	55.340	1602.5(23.20)‡	1531.0	0.462
r102	1194.8	18641.9	1268.1(11.38)	1255.1	59.620	1403.6(37.67)‡	1338.2	0.399
r103	-	-	1113.8(13.83)	1099.9	59.500	1238.6(18.60)‡	1189.6	0.385
r104	-	-	975.0(4.40)	970.2	63.320	1065.7(15.82)‡	1027.3	0.325
r105	1171.2	3780.2	1267.7(7.55)	1256.3	59.140	1301.0(1.14)‡	1298.5	0.413
r106	-	-	1139.5(6.29)	1124.1	59.260	1257.1(29.45)‡	1205.4	0.366
r107	995.3	5164.6	1034.4(8.05)	1025.5	62.400	1151.1(29.71)‡	1085.9	0.380
r108	-	-	946.5(5.93)	942.0	61.810	1012.9(17.46)‡	975.5	0.325
r109	1045.7	13239.2	1086.0(12.05)	1072.9	51.530	1194.0(33.40)‡	1124.5	0.408
r110	-	-	1042.5(5.24)	1034.9	52.480	1120.8(10.02)‡	1083.3	0.370
r111	-	-	1010.1(11.83)	1004.8	55.735	1132.1(44.24)‡	1053.0	0.358
r112	937.1	28734.1	957.6(2.41)	956.4	55.550	1028.7(15.64)‡	990.8	0.369
w-d-1	6-0-6	-	-	-	-	12-0-0	-	-
No.best	6	-	0	6	-	0	0	-
Ave.PDR	0.00%	-	3.05%	-	-	12.26%	-	-
Ave.Time	-	12337.883	-	-	57.974	-	-	0.380

Table 6: Results on the *gdb* benchmark test set in the 3LP in terms of costs of solutions. For each instance, the average performance of an algorithm is indicated in bold if it is the best among all comparison algorithms. “‡” and “†” indicate MAENS-GN performs significantly better than and equivalently to the corresponding algorithm based on 20 independent runs according to the Wilcoxon rank-sum test with significant level $p = 0.05$, respectively.

Instances	R	LB	MAENS	MAENS-GN				VND	VND-GN				VND-GN*	
				Ave	Ave(std)	Best	Time		Ave	Ave(std)	Best	Time	Ave(std)	Best
gdb1	22	316	2510.0	618.5(0.90)	617.4	43.850	2510.0	618.5(0.76)†	617.7	10.310	617.9(0.51)	617.2		
gdb2	26	339	2132.0	622.4(0.92)	621.2	65.591	2143.8	631.8(12.98)‡	621.1	12.730	627.6(10.27)†	621.0		
gdb3	22	275	634.0	289.0(0.00)	289.0	6.703	698.9	331.7(30.21)‡	311.0	0.098	312.2(5.45)‡	311.0		
gdb4	19	287	4641.0	745.5(0.88)	744.4	49.972	4641.0	745.8(0.97)†	744.1	11.488	745.1(0.54)†	744.3		
gdb5	26	377	426.6	389.6(9.22)	377.5	9.601	452.8	416.5(9.95)‡	396.5	0.125	403.8(7.06)‡	391.0		
gdb6	22	298	2526.0	572.9(14.64)	562.3	37.047	2596.9	593.5(25.46)‡	539.3	8.065	579.3(29.16)†	538.7		
gdb7	22	325	507.2	468.0(3.82)	459.4	28.250	547.7	497.6(17.55)‡	468.9	6.823	486.7(12.32)‡	467.4		
gdb8	46	348	525.7	391.7(11.09)	368.8	39.971	550.5	439.5(6.43)‡	411.5	0.655	397.5(13.44)†	383.0		
gdb9	51	303	1056.5	319.8(10.18)	309.0	46.583	1145.0	413.2(31.61)‡	348.0	0.899	353.0(10.63)‡	334.0		
gdb10	25	275	340.2	286.6(11.19)	275.0	8.081	370.2	321.2(3.97)‡	318.0	0.117	313.9(7.34)‡	294.0		
gdb11	45	395	759.9	417.5(5.36)	411.0	39.611	856.6	468.3(17.18)‡	439.0	0.625	436.2(10.30)‡	417.0		
gdb12	23	458	925.4	479.4(25.84)	458.0	9.007	1020.8	577.6(26.76)‡	540.0	0.088	533.8(12.06)‡	520.0		
gdb13	28	536	705.2	615.1(3.39)	609.8	31.838	740.9	643.8(13.52)‡	621.1	8.240	641.6(14.78)‡	620.6		
gdb14	21	100	342.2	167.5(6.13)	154.8	7.418	353.1	169.8(10.18)†	141.8	0.081	155.2(7.85)	140.4		
gdb15	21	58	2826.0	79.5(1.52)	76.8	43.215	2827.7	79.8(1.24)†	77.2	5.389	78.2(1.06)	76.2		
gdb16	28	127	152.2	137.1(2.61)	133.1	11.062	155.9	138.2(0.00)†	138.2	0.159	138.2(0.00)†	138.2		
gdb17	28	91	3897.8	113.3(1.50)	109.9	50.624	3900.6	112.7(1.26)†	111.3	9.821	111.7(0.28)	111.3		
gdb18	36	164	618.6	167.6(3.34)	164.0	16.700	641.0	192.9(12.65)‡	172.0	0.327	175.8(5.03)‡	166.0		
gdb19	11	55	134.0	60.0(0.00)	60.0	2.045	145.4	68.6(10.29)‡	55.0	0.022	61.5(7.67)†	55.0		
gdb20	22	121	269.2	129.4(3.92)	124.0	7.272	309.8	146.5(20.27)‡	127.0	0.080	129.3(2.24)†	126.0		
gdb21	33	156	528.1	258.2(11.32)	239.5	18.885	536.9	262.4(3.74)‡	249.6	0.330	250.1(8.09)	236.9		
gdb22	44	200	593.6	317.7(9.57)	298.5	39.338	599.8	308.2(0.14)	308.1	0.750	307.9(1.04)	303.4		
gdb23	55	233	839.3	346.8(8.51)	335.6	71.849	813.2	337.4(0.00)	337.4	1.690	337.4(0.00)	337.4		
w-d-1	-	-	-	-	-	-	-	15-6-2	-	-	9-7-7	-		
No.best	-	-	-	1	18	-	-	0	5	-	0	8		
Ave.PDR	-	-	638.86%	37.38%	-	-	649.94%	45.22%	-	-	39.27%	-		
Ave.Time	-	-	-	-	-	29.761	-	-	-	3.431	-	-		

modified here to handle the instances (except Solomon’s test set) of CARPTDSC under time-dependent service time.

The metrics are those commonly used in the literature of vehicle/arc routing [44–48] and are divided into two categories.

One is the metric for evaluating the solution quality, including w-d-1, No.best and Ave.PDR. The other is the time metric, namely Ave.Time [44]. w-d-1 refers to the number of instances on which the proposed algorithm is superior to, not significantly

different from, or inferior to the corresponding compared algorithm in the test set. The comparison is based on the average value of 20 independent repeated experiments, and the wilcoxon ranksum test [49] with the significance level $p = 0.05$ was employed here. No.best refers to the number of instances where the algorithm reaches the best value in the test set. The best value refers to the optimal result achieved by all comparison algorithms on that instance in 20 independent runs. Note that No.best, unless otherwise specified, refers to the data in the column headed Best in the tables, even though No.best has also data in the columns headed Ave(std). Ave.PDR refers to the value of the average performance degradation ratio (PDR) of the algorithm over all instances in the instance set. PDR is calculated as $(TC_1 - TC_2)/TC_2 * 100\%$, where TC_1 is the average cost value of the algorithm on that instance, and TC_2 is the lower bound or the best value of all compared algorithms on that instance. Ave.Time refers to the average time spent by the algorithm on all instances in this test set. Therefore, the smaller the values of Ave.PDR and Ave.Time, the better.

In Tables 1-9, the columns headed Ave(std), Best, and Time stand for average results (standard deviations), best results, and average computation time (in seconds) over 20 independent runs, respectively. In addition, the columns headed $|R|$ provide the number of tasks in the instances. According to the method in [9], the lower bounds of *gdb* and *egl* in the static test set are still the lower bounds of *gdb* and *egl* in the 2LP and 3LP. Therefore the columns headed LB provide the lower bounds found so far for the instances, which were collected from [2, 9, 22, 19, 50–52].

4.2. Results related to RQ1

This section is mainly to verify whether MAENS-GN significantly improves the solution quality on the test sets in the 2LP.

From Tables 1-2 and the solution quality metrics, i.e., w-d-l, No.best and Ave.PDR, it can be seen that MAENS-GN is significantly better than VND in terms of average values, best values and proximity to the lower bounds on the small-scale *gdb* and larger-scale *egl* test sets in the 2LP. For example, the w-d-l value of VND on the *gdb* set in the 2LP is 23-0-0, which means that the average values of MAENS-GN on all 23 instances of the *gdb* set in the 2LP are significantly better than those of VND. However, for Ave.Time, MAENS-GN is more time-consuming than VND. For a fairer comparison, VND* also participated in the comparison. It can be seen from Tables 1-2 that when VND runs for more time, i.e., the runtime of MAENS-GN, the effect becomes better. For instance, on the *gdb* set in the 2LP, the Ave.PDR values of VND and VND* are 10.82% and 8.74%, respectively, which is an improvement of 2.08%. However, MAENS-GN still maintains its superiority. The small standard deviation values for MAENS-GN indicate good robustness.

The experiments reveal that MAENS-GN significantly outperforms VND and VND* on both small-scale *gdb* test set and larger-scale *egl* test set for w-d-l, No.best, and Ave.PDR, suggesting that MAENS-GN significantly improves the solution quality in the 2LP. The main reason why MAENS-GN can outperform VND and VND* may be that the search performance

of MAENS is better than that of VND. The inclusion of various search operators, such as Merge-split, helps to improve the performance of MAENS-GN. In addition, the novel initialization method makes the effect better. However, it is noted that MAENS-GN is more time-consuming than VND, primarily due to the higher time complexity of operators like Merge-split.

4.3. Results related to RQ2

This section mainly verifies the performance of MAENS-GN on both small-scale and larger-scale instances in the 3LP. Additionally, the contribution of GSS and NCS to the performance of MAENS-GN is examined.

Because the comparison algorithms were run on different computers, the runtime needs to be normalized. So about the time values of CG, they were converted according to the types of computers. The computer processor used for CG in [8] was the 400 MHz UltraSparc II, while the computer used for MAENS-GN and VND-GN was Intel(R) Xeon(R) Platinum 9242 CPU @ 2.30GHz. To make a fair comparison, all the time values of CG in [8] were divided by 5.75 (i.e., 2.3GHz/400MHz), then added to Tables 3-5. In Table 5, CG could not get results on many instances due to memory or time constraints, denoted by “-”. These instances are not involved in the calculation, such as Ave.PDR and Ave.Time. Although CG, being an exact algorithm, outperforms MAENS-GN in terms of the solution quality (since CG can find optimal solutions), MAENS-GN significantly reduces runtime. For example, the average runtimes of CG and MAENS-GN on *Solomon-25* were 626.115 and 13.875, respectively, which results in a reduction of approximately 45 times in runtime. The reason why MAENS-GN is faster than CG is mainly because MAENS-GN is a stochastic approximate algorithm, which only needs to get some good approximate and feasible solutions. While CG is an exact algorithm, which needs to find the optimal solution, the search accuracy and time complexity are generally higher. Therefore, the search speed of MAENS-GN is generally faster.

As can be seen from Tables 3-8, in terms of solution quality metrics w-d-l, No.best, and Ave.PDR, MAENS-GN is significantly better than VND-GN in the *Solomon-25*, *Solomon-35*, *Solomon-40*, *gdb*, *egl* and, real-world *jd* test sets in the 3LP. For example, on the *jd* set, the w-d-l value of VND-GN is 16-0-0, indicating that the average values of MAENS-GN on all 16 instances in the *jd* set are significantly better than those of VND-GN. However on Ave.Time, MAENS-GN is worse than VND-GN. For a fairer comparison, VND-GN* is compared on the small-scale *gdb* test set and the larger-scale *egl* test set in the 3LP in Tables 6-7. It can be seen that as the runtime increases, the performance of VND-GN improves. For example, on the *gdb* set in the 3LP in Table 6, the Ave.PDR values of VND-GN and VND-GN* are 45.22% and 39.27%, respectively, which indicates an improvement of about 6%. Despite this improvement, MAENS-GN remains better than VND-GN*.

In the comparison between MAENS and MAENS-GN, as well as between VND and VND-GN, presented in Tables 6-7, it is observed that GSS and NCS have greatly improved the performance of both MAENS and VND. For example, it can be seen from Table 6 that the Ave.PDR values of MAENS

Table 7: Results on the *egl* benchmark test set in the 3LP in terms of costs of solutions. For each instance, the average performance of an algorithm is indicated in bold if it is the best among all comparison algorithms. “‡” and “†” indicate MAENS-GN performs significantly better than and equivalently to the corresponding algorithm based on 20 independent runs according to the Wilcoxon rank-sum test with significant level $p = 0.05$, respectively.

Instances	R	LB	MAENS			MAENS-GN			VND			VND-GN			VND-GN*		
			Ave	Ave(std)	Best	Time	Ave	Best	Time	Ave	Best	Time	Ave(std)	Best	Time	Ave(std)	Best
egl-e1-A	51	3548	3669.0	3588.2(7.59)	3569.3	98.445	3909.3	3867.4(0.00)‡	3867.4	0.885	3858.7(17.75)‡	3867.4	0.885	3858.7(17.75)‡	3817.7		
egl-e1-B	51	4498	4846.4	4582.2(42.20)	4498.0	80.793	5263.0	4927.8(76.50)‡	4694.0	0.928	4689.2(36.57)‡	4694.0	0.928	4689.2(36.57)‡	4628.0		
egl-e1-C	51	5595	6343.0	5895.6(62.65)	5737.8	110.685	6523.0	6125.8(21.57)‡	6104.7	14.903	6092.4(36.51)‡	6104.7	14.903	6092.4(36.51)‡	5978.7		
egl-e2-A	72	5018	5102.5	5056.4(50.04)	5018.0	200.536	5217.3	5180.0(0.00)‡	5180.0	2.729	5180.0(0.00)‡	5180.0	2.729	5180.0(0.00)‡	5180.0		
egl-e2-B	72	6317	6536.8	6377.4(22.60)	6350.0	179.683	6763.0	6605.0(0.00)‡	6605.0	2.420	6577.1(38.09)‡	6605.0	2.420	6577.1(38.09)‡	6459.0		
egl-e2-C	72	8335	8560.1	8500.3(98.31)	8365.5	164.139	8710.5	8699.0(0.00)‡	8699.0	2.388	8694.4(20.05)‡	8699.0	2.388	8694.4(20.05)‡	8607.0		
egl-e3-A	87	5898	6238.9	6091.9(99.65)	5924.0	335.173	6641.0	6425.0(48.17)‡	6215.0	4.426	6380.5(71.48)‡	6215.0	4.426	6380.5(71.48)‡	6215.0		
egl-e3-B	87	7744	8499.4	8285.4(137.10)	8077.6	306.216	8930.0	8911.9(35.90)‡	8820.8	19.488	8776.2(76.53)‡	8820.8	19.488	8776.2(76.53)‡	8576.9		
egl-e3-C	87	10244	10527.8	10404.0(61.50)	10345.0	238.743	11254.2	11109.8(151.15)‡	10684.0	3.773	10699.8(68.17)‡	10684.0	3.773	10699.8(68.17)‡	10469.0		
egl-e4-A	98	6408	7263.7	7036.9(112.66)	6839.3	392.461	7698.9	7698.9(22.23)‡	7602.0	29.410	7212.6(11.57)‡	7602.0	29.410	7212.6(11.57)‡	7163.3		
egl-e4-B	98	8935	9240.3	9190.4(57.97)	9109.1	336.769	9838.5	9805.5(109.47)‡	9497.4	6.320	9545.8(62.31)‡	9497.4	6.320	9545.8(62.31)‡	9416.8		
egl-e4-C	98	11512	12929.1	12362.4(236.91)	12088.7	301.267	13007.0	12376.3(162.53)‡	12201.7	56.897	12532.7(235.41)‡	12201.7	56.897	12532.7(235.41)‡	12038.1		
egl-s1-A	75	5018	5193.9	5120.0(51.02)	5058.0	227.150	5603.5	5530.0(0.00)‡	5530.0	3.049	5398.1(70.41)‡	5530.0	3.049	5398.1(70.41)‡	5272.5		
egl-s1-B	75	6388	7853.6	7080.4(247.18)	6845.0	251.313	8158.6	7734.0(295.17)‡	6789.7	50.189	7504.6(206.84)‡	6789.7	50.189	7504.6(206.84)‡	6915.9		
egl-s1-C	75	8518	12900.2	10635.6(292.52)	10015.3	255.124	12582.0	10318.0(475.28)	10009.0	72.490	10616.9(447.63)‡	10009.0	72.490	10616.9(447.63)‡	9632.6		
egl-s2-A	147	9825	10778.6	10668.1(89.07)	10454.1	1154.471	11633.2	11621.1(92.39)‡	11243.2	75.050	11265.9(103.77)‡	11243.2	75.050	11265.9(103.77)‡	11084.7		
egl-s2-B	147	13017	13702.2	13562.7(65.58)	13464.0	800.752	14256.0	14071.0(0.00)‡	14071.0	16.248	14069.1(8.28)‡	14071.0	16.248	14069.1(8.28)‡	14033.0		
egl-s2-C	147	16425	19320.3	18521.3(402.58)	17700.4	873.643	20029.2	19605.6(621.87)‡	18350.2	117.071	18917.6(248.39)‡	18350.2	117.071	18917.6(248.39)‡	1850.02		
egl-s3-A	159	10165	10913.8	10901.3(68.05)	10756.0	1456.500	11600.8	11593.9(14.27)‡	11556.0	84.768	11549.6(33.82)‡	11556.0	84.768	11549.6(33.82)‡	11418.0		
egl-s3-B	159	13648	14383.7	14140.5(57.27)	14026.5	1052.030	14834.7	14586.1(0.00)‡	14586.1	25.311	14586.1(0.00)‡	14586.1	25.311	14586.1(0.00)‡	14586.1		
egl-s3-C	159	17188	18118.1	18112.5(137.87)	17847.0	976.738	19221.0	19220.7(146.84)‡	18816.0	113.329	19019.5(132.41)‡	18816.0	113.329	19019.5(132.41)‡	18778.0		
egl-s4-A	190	12153	13170.0	12827.4(141.70)	12640.0	1534.158	13763.0	13355.0(0.00)‡	13355.0	31.805	13355.0(0.00)‡	13355.0	31.805	13355.0(0.00)‡	13355.0		
egl-s4-B	190	16113	17122.4	16831.0(122.39)	16643.0	1550.589	17880.0	17647.0(0.00)‡	17647.0	36.325	17531.8(131.39)‡	17647.0	36.325	17531.8(131.39)‡	17176.0		
egl-s4-C	190	20430	21423.3	21281.8(88.73)	21083.0	1380.502	21080.8	20920.4(0.00)‡	20920.4	42.440	20915.0(23.69)	20920.4	42.440	20915.0(23.69)	20811.7		
w-d1	-	-	-	-	-	-	-	21-1-2	-	-	22-1-1	-	-	-	-	-	-
No.best	-	-	-	0	21	-	-	1	3	-	0	-	-	3	-	-	-
Ave.PDR	-	-	9.50%	5.74%	-	-	14.14%	10.95%	-	-	9.48%	-	-	-	-	-	-
Ave.Time	-	-	-	-	-	594.078	-	-	-	33.86	-	-	-	-	-	-	-

Table 8: Results on the *jd* benchmark test set in the 3LP in terms of costs of solutions. For each instance, the average performance of an algorithm is indicated in bold if it is the best among all comparison algorithms. “‡” and “†” indicate MAENS-GN performs significantly better than and equivalently to the corresponding algorithm based on 20 independent runs according to the Wilcoxon rank-sum test with significant level $p = 0.05$, respectively.

Instances	R	MAENS-GN			VND-GN		
		Ave(std)	Best	Time	Ave(std)	Best	Time
jd-50-1	50	3268.2(11.80)	3252.8	79.554	3386.7(18.44)‡	3334.1	1.872
jd-50-2	50	3593.8(32.80)	3546.0	87.707	3690.6(40.37)‡	3612.0	10.185
jd-50-3	50	3363.5(8.92)	3342.0	51.834	3484.1(37.69)‡	3423.0	1.677
jd-50-4	50	3580.2(28.08)	3514.1	50.784	3710.0(38.18)‡	3672.0	9.003
jd-100-1	100	6234.8(18.29)	6211.0	569.377	6411.4(47.80)‡	6348.0	18.275
jd-100-2	100	6186.2(25.71)	6117.0	555.759	6383.2(55.38)‡	6308.0	17.363
jd-100-3	100	5876.3(33.83)	5822.2	561.251	6194.8(48.66)‡	6088.2	13.642
jd-100-4	100	6280.4(33.85)	6213.0	552.321	6467.9(67.47)‡	6317.0	16.815
jd-150-1	150	8992.4(36.63)	8916.9	1584.547	9316.4(74.51)‡	9186.0	97.842
jd-150-2	150	9298.0(56.46)	9188.0	1598.263	9712.7(54.72)‡	9605.0	106.934
jd-150-3	150	9277.6(63.22)	9131.0	1544.837	9644.1(84.76)‡	9453.6	95.801
jd-150-4	150	9188.0(40.36)	9080.0	1479.287	9380.8(88.57)‡	9205.0	62.927
jd-200-1	200	10865.5(52.49)	10755.4	3260.699	11442.5(116.23)‡	11074.9	114.503
jd-200-2	200	10866.2(45.73)	10770.1	3311.978	11351.7(72.46)‡	11190.3	122.243
jd-200-3	200	11727.0(35.86)	11658.0	3018.696	12117.7(124.04)‡	11870.6	225.431
jd-200-4	200	11529.8(52.23)	11440.0	3052.575	11767.8(107.15)‡	11593.0	135.499
w-d-1	-	-	-	-	16-0-0	-	-
No.best	-	0	16	-	0	-	-
Ave.PDR	-	0.00%	-	-	3.58%	-	-
Ave.Time	-	-	-	1334.967	-	-	65.626

and MAENS-GN are 638.86% and 37.38%, respectively, which indicates that GSS and NCS improved MAENS by about 17 times. It can also be seen that the difference between MAENS-GN and VND-GN is almost equal to the difference between MAENS and VND on Ave.PDR. For example, on the *egl* set in the 3LP in Table 7, the Ave.PDR values of VND-GN and MAENS-GN are 10.95% and 5.74%, respectively, and the difference is 5.21%. The Ave.PDR values of VND and MAENS are 14.14% and 9.50%, respectively, and the difference is 4.64%. This shows that the reason why MAENS-GN is better than VND-GN is largely due to the fact that MAENS is better than VND.

In summary, MAENS-GN demonstrates excellent results across the small-scale, larger-scale, or real-world test sets in the 3LP. Moreover, GSS and NCS have greatly enhanced the performance of MAENS-GN.

4.4. Effectiveness of the novel initialization strategy

This section aims to investigate a question: Is the novel initialization strategy in MAENS superior to the original initialization strategy? Here, two algorithms are compared, namely MAENS with the original initialization strategy (here represented as MAENS) and MAENS with the novel initialization strategy (here represented as MAENS*). The larger-scale *egl* test set in the 2LP was used. Ave.CD and Ave.PDR were used as the metrics on the test set. Ave.CD represents the average CD on all instances. CD, representing the cost difference from the lower bound (i.e., LB) on an instance, is expressed as $CD = (cost - LB)$.

In Table 9, the Ave.CD values of MAENS* and MAENS are 482.28 and 498.18, respectively, with a difference of 15.9. This

observation indicates that the novel initialization strategy enhances the cost value of the algorithm by 15.9 on each instance on average. Turning to Ave.PDR, the values of MAENS* and MAENS are 4.18% and 4.32%, respectively, with a difference of 0.14%. This shows that the novel initialization strategy improves the algorithm by 0.14% on Ave.PDR.

Through the aforementioned experiments, it is evident that, on the larger-scale *egl* test set in the 2LP, the novel initialization strategy has visible improvements to the proposed algorithm in terms of the average costs of the solutions. However, experiments, conducted on the small-scale *gdb* test set in the 2LP, did not exhibit substantial improvement with the novel initialization strategy, and the results are not presented here. The main reason behind this observation may be that, as the number of the tasks increases, the quality of the initialized solutions deteriorates when using the original initialization strategy. MAENS with the original initialization strategy already demonstrates satisfactory results on the small-scale *gdb* test set in the 2LP, making the impact of the operation for the time-dependent characteristics less apparent. However, on the larger-scale *egl* test set, the effectiveness of the original initialization strategy diminishes. At this time, the incorporation of targeted operations for time-dependent characteristics proves to enhance the effect of the initialization strategy. It is worth mentioning why experiments were not conducted on the test sets in the 3LP, such as the *gdb* and *egl* sets in the 3LP. One reason is due to space limitations. Of course, the main reason is that the original/novel initialization strategy is embedded in the algorithm in the first stage of MAENS-GN, i.e., MAENS, and assessing the effect of MAENS provides a more direct perspective. Additionally, as indicated in Section 4.3, the superiority of MAENS-GN over

Table 9: Comparison between MAENS* and MAENS on the *egl* benchmark test set in the 3LP in terms of costs of solutions.

Instances	R	LB	MAENS*	MAENS	Instances	R	LB	MAENS*	MAENS
egl-e1-A	51	3548	3550.6	3549.2	egl-s1-A	75	5018	5145.9	5178.2
egl-e1-B	51	4498	4576.9	4575.7	egl-s1-B	75	6388	6576.6	6576.6
egl-e1-C	51	5595	5677.6	5679.8	egl-s1-C	75	8518	8783.8	8803.6
egl-e2-A	72	5018	5102.4	5116.9	egl-s2-A	147	9825	10490.1	10514.6
egl-e2-B	72	6317	6424.9	6442.9	egl-s2-B	147	13017	13887.2	13903.4
egl-e2-C	72	8335	8599.0	8597.1	egl-s2-C	147	16425	17392.6	17399.6
egl-e3-A	87	5898	6099.4	6047.4	egl-s3-A	159	10165	10733.0	10800.9
egl-e3-B	87	7744	8040.6	8032.0	egl-s3-B	159	13648	14418.0	14490.4
egl-e3-C	87	10244	10460.6	10462.4	egl-s3-C	159	17188	18269.3	18279.0
egl-e4-A	98	6408	6710.6	6729.0	egl-s4-A	190	12153	13197.1	13193.5
egl-e4-B	98	8935	9329.9	9337.2	egl-s4-B	190	16113	17260.1	17302.6
egl-e4-C	98	11512	11992.6	12004.3	egl-s4-C	190	20430	21796.0	21880.0
Ave.CD	-	-	-	-	-	-	-	482.28	498.18
Ave.PDR	-	-	-	-	-	-	-	4.18%	4.32%

VND-GN is primarily attributed to the superiority of MAENS over VND. This insight suggests that an improvement in the effect of MAENS generally leads to the improvement of performance of MAENS-GN on the test sets in the 3LP. Therefore, it is not really necessary to conduct experiments on the test sets in the 3LP either.

5. Conclusion and future work

Experiments were conducted on the modified standard test sets and a real-world test set, which demonstrates excellent results for MAENS-GN. Specifically, the proposed algorithm, i.e., MAENS-GN, has effectively addressed two research questions, which indicates that two existing limitations are addressed in this field.

In the optimization of the vehicle departure time, this paper conducts a detailed analysis of the relationship between the route cost and the vehicle departure time in various scenarios. Based on the analyzed relationship, tailored methods are employed in different scenarios to optimize the vehicle departure time, which thereby avoids the waste of calculation time and lack of accuracy of the obtained departure time caused by using a uniform method. Furthermore, in the routing stage, a specialized operation for time-dependent characteristics is introduced to the initialization strategy to improve its effectiveness.

Despite its significant advantages, MAENS-GN also has some shortcomings. Firstly, MAENS-GN exhibits high time consumption. Secondly, although many solutions obtained by MAENS-GN reach the lower bounds of the instances in the 2LP, there remains a discernible gap from the lower bounds of the instances in the 3LP. Consequently, our next work focuses on reducing the time consumption of the algorithm and enhancing the solution quality in the 3LP. One way to improve solution quality in the 3LP can be as follows. With the reduction of time consumption of MAENS-GN, the algorithms in the two stages of MAENS-GN, i.e., MAENS and GSS (or NCS), can be iterated multiple times to further enhance the quality of the solutions in the 3LP.

References

- [1] X. Jin, H. Qin, Z. Zhang, M. Zhou, J. Wang, Planning of garbage collection service: An arc-routing problem with time-dependent penalty cost, *IEEE Transactions on Intelligent Transportation Systems* 22 (5) (2020) 2692–2705.
- [2] K. Tang, Y. Mei, X. Yao, Memetic algorithm with extended neighborhood search for capacitated arc routing problems, *IEEE Transactions on Evolutionary Computation* 13 (5) (2009) 1151–1166.
- [3] H. Handa, L. Chapman, X. Yao, Robust route optimization for gritting/salting trucks: A cercia experience, *IEEE Computational Intelligence Magazine* 1 (1) (2006) 6–9.
- [4] L. Bodin, G. Fagin, R. Weleby, J. Greenberg, The design of a computerized sanitation vehicle routing and scheduling system for the town of oyster bay, new york, *Computers & Operations Research* 16 (1) (1989) 45–54.
- [5] P. Lacomme, C. Prins, W. Ramdane-Chérif, Evolutionary algorithms for periodic arc routing problems, *European Journal of Operational Research* 165 (2) (2005) 535–553.
- [6] L. D. Bodin, S. J. Kursh, A computer-assisted system for the routing and scheduling of street sweepers, *Operations Research* 26 (4) (1978) 525–537.
- [7] H. I. Stern, M. Dror, Routing electric meter readers, *Computers & Operations Research* 6 (4) (1979) 209–223.
- [8] M. Tagmouti, M. Gendreau, J.-Y. Potvin, Arc routing problems with time-dependent service costs, *European Journal of Operational Research* 181 (1) (2007) 30–39.
- [9] M. Tagmouti, M. Gendreau, J.-Y. Potvin, A variable neighborhood descent heuristic for arc routing problems with time-dependent service costs, *Computers & Industrial Engineering* 59 (4) (2010) 954–963.
- [10] M. Tagmouti, M. Gendreau, J.-Y. Potvin, A dynamic capacitated arc routing problem with time-dependent service costs, *Transportation Research Part C: Emerging Technologies* 19 (1) (2011) 20–28.
- [11] K. OVERHOLT, Fibonacci search - minx and golden section search, *COMPUTER JOURNAL* 9 (4) (1967) 414–&.
- [12] K. Tang, P. Yang, X. Yao, Negatively correlated search, *IEEE Journal on Selected Areas in Communications* 34 (3) (2016) 542–550.
- [13] E. Dijkstra, A note on two papers in connection with graphs, *Numerische Mathematik* (1959) 1–269.
- [14] B. L. Golden, R. T. Wong, Capacitated arc routing problems, *Networks* 11 (3) (1981) 305–315.
- [15] N. Christofides, The optimum traversal of a graph, *Omega* 1 (6) (1973) 719–732.
- [16] B. L. Golden, J. S. DeArmon, E. K. Baker, Computational experiments with algorithms for a class of routing problems, *Computers & Operations Research* 10 (1) (1983) 47–59.
- [17] A. Hertz, G. Laporte, M. Mittaz, A tabu search heuristic for the capacitated arc routing problem, *Operations research* 48 (1) (2000) 129–135.
- [18] A. Hertz, M. Mittaz, A variable neighborhood descent algorithm for the

- undirected capacitated arc routing problem, *Transportation science* 35 (4) (2001) 425–434.
- [19] P. Beullens, L. Muyldermans, D. Cattrysse, D. Van Oudheusden, A guided local search heuristic for the capacitated arc routing problem, *European Journal of Operational Research* 147 (3) (2003) 629–643.
- [20] H. Handa, D. Lin, L. Chapman, X. Yao, Robust solution of salting route optimisation using evolutionary algorithms, in: 2006 IEEE International Conference on Evolutionary Computation, IEEE, 2006, pp. 3098–3105.
- [21] P. Lacomme, C. Prins, W. Ramdane-Cherif, Competitive memetic algorithms for arc routing problems, *Annals of Operations Research* 131 (2004) 159–185.
- [22] T. Vidal, Node, edge, arc routing and turn penalties: Multiple problems—one neighborhood extension, *Operations Research* 65 (4) (2017) 992–1010.
- [23] H. Longo, M. P. De Aragao, E. Uchoa, Solving capacitated arc routing problems using a transformation to the cvrp, *Computers & Operations Research* 33 (6) (2006) 1823–1837.
- [24] W.-L. Pearn, A. Assad, B. L. Golden, Transforming arc routing into node routing problems, *Computers & operations research* 14 (4) (1987) 285–288.
- [25] C. Malandraki, M. S. Daskin, Time dependent vehicle routing problems: Formulations, properties and heuristic algorithms, *Transportation science* 26 (3) (1992) 185–200.
- [26] H.-K. Chen, C.-F. Hsueh, M.-S. Chang, The real-time time-dependent vehicle routing problem, *Transportation Research Part E: Logistics and Transportation Review* 42 (5) (2006) 383–408.
- [27] S. Dabia, S. Ropke, T. Van Woensel, T. De Kok, Branch and price for the time-dependent vehicle routing problem with time windows, *Transportation science* 47 (3) (2013) 380–396.
- [28] G. Kim, Y. S. Ong, T. Cheong, P. S. Tan, Solving the dynamic vehicle routing problem under traffic congestion, *IEEE Transactions on Intelligent Transportation Systems* 17 (8) (2016) 2367–2380.
- [29] M. Soysal, M. Çimen, A simulation based restricted dynamic programming approach for the green time dependent vehicle routing problem, *Computers & Operations Research* 88 (2017) 297–305.
- [30] A. Haghani, S. Jung, A dynamic vehicle routing problem with time-dependent travel times, *Computers & operations research* 32 (11) (2005) 2959–2986.
- [31] S. R. Balseiro, I. Loiseau, J. Ramonet, An ant colony algorithm hybridized with insertion heuristics for the time dependent vehicle routing problem with time windows, *Computers & Operations Research* 38 (6) (2011) 954–966.
- [32] E. Yao, Z. Lang, Y. Yang, Y. Zhang, Vehicle routing problem solution considering minimising fuel consumption, *IET Intelligent Transport Systems* 9 (5) (2015) 523–529.
- [33] H. Tong, L. L. Minku, S. Menzel, B. Sendhoff, X. Yao, A hybrid local search framework for the dynamic capacitated arc routing problem, in: *Proceedings of the Genetic and Evolutionary Computation Conference Companion*, 2021, pp. 139–140.
- [34] J. Sun, G. Tan, G. Hou, A new integer programming formulation for the chinese postman problem with time dependent travel times, *International Journal of Computer and Information Engineering* 5 (4) (2011) 410–414.
- [35] D. Black, R. Eglese, S. Wöhlk, The time-dependent prize-collecting arc routing problem, *Computers & Operations Research* 40 (2) (2013) 526–535.
- [36] J. Nossack, B. Golden, E. Pesch, R. Zhang, The windy rural postman problem with a time-dependent zigzag option, *European Journal of Operational Research* 258 (3) (2017) 1131–1142.
- [37] T. Calogiuri, G. Ghiani, E. Guerriero, R. Mansini, A branch-and-bound algorithm for the time-dependent rural postman problem, *Computers & Operations Research* 102 (2019) 150–157.
- [38] C. Ahabchane, A. Langevin, M. Trépanier, The mixed capacitated general routing problem with time-dependent demands, *Networks* 76 (4) (2020) 467–484.
- [39] T. Vidal, R. Martinelli, T. A. Pham, M. H. Hà, Arc routing with time-dependent travel times and paths, *Transportation Science* 55 (3) (2021) 706–724.
- [40] J. H. Holland, *Adaptation in Natural and Artificial Systems*, University of Michigan Press, 1975.
- [41] J. S. DeArmon, A comparison of heuristics for the capacitated chinese postman problem, Ph.D. thesis, University of Maryland (1981).
- [42] R. W. Eglese, Routeing winter gritting vehicles, *Discrete applied mathematics* 48 (3) (1994) 231–244.
- [43] M. M. Solomon, Algorithms for the vehicle routing and scheduling problems with time window constraints, *Operations research* 35 (2) (1987) 254–265.
- [44] S. Liu, K. Tang, X. Yao, Memetic search for vehicle routing with simultaneous pickup-delivery and time windows, *Swarm and Evolutionary Computation* 66 (2021) 100927.
- [45] S. Liu, P. Yang, K. Tang, Approximately optimal construction of parallel algorithm portfolios by evolutionary intelligence, *SCIENTIA SINICA Technologica* 53 (2) (2023) 280–290. doi:<https://doi.org/10.1360/SST-2021-0372>.
- [46] S. Liu, K. Tang, X. Yao, Generative adversarial construction of parallel portfolios, *IEEE Transactions on Cybernetics* 52 (2) (2022) 784–795.
- [47] K. Tang, S. Liu, P. Yang, X. Yao, Few-shots parallel algorithm portfolio construction via co-evolution, *IEEE Transactions on Evolutionary Computation* 25 (3) (2021) 595–607.
- [48] S. Liu, Y. Zhang, K. Tang, X. Yao, How good is neural combinatorial optimization? A systematic evaluation on the traveling salesman problem, *IEEE Computational Intelligence Magazine* 18 (3) (2023) 14–28.
- [49] F. Wilcoxon, Individual comparisons by ranking methods, in: *Breakthroughs in Statistics: Methodology and Distribution*, Springer, 1992, pp. 196–202.
- [50] J. Brandão, R. Eglese, A deterministic tabu search algorithm for the capacitated arc routing problem, *Computers & Operations Research* 35 (4) (2008) 1112–1126.
- [51] J. M. Belenguer, E. Benavent, A cutting plane algorithm for the capacitated arc routing problem, *Computers & Operations Research* 30 (5) (2003) 705–728.
- [52] D. Ahr, Contributions to multiple postmen problems, Ph.D. thesis (2004).